PHYSICAL REVIEW B

CONDENSED MATTER AND MATERIALS PHYSICS

THIRD SERIES, VOLUME 58, NUMBER 23 **15 DECEMBER 1998-I**

BRIEF REPORTS

Brief Reports are accounts of completed research which, while meeting the usual **Physical Review B** *standards of scientific quality, do not warrant regular articles. A Brief Report may be no longer than four printed pages and must be accompanied by an abstract. The same publication schedule as for regular articles is followed, and page proofs are sent to authors.*

Long-wavelength optical phonons in ternary nitride-based crystals

SeGi Yu and K. W. Kim
Department of Electrical and Computer Engineering, North Carolina State University, Raleigh, North Carolina 27695-7911

Leah Bergman
Department of Physics, North Carolina State University, Raleigh, North Carolina 27695-8202

Mitra Dutta, Michael A. Stroscio, and John M. Zavada
U.S. Army Research Office, P.O. Box 12211, Research Triangle Park, North Carolina 27709-2211

(Received 21 May 1998)

Phonon modes in column-III–nitride ternary semiconductors are investigated theoretically within the modified random-element isodisplacement model. It is found that A_1 and E_1 branches of optical phonons in wurtzite $Ga_xAl_{1-x}N$ and $In_xGa_{1-x}N$ exhibit one-mode behavior. This result is explained by the fact that atomic mass of nitrogen is much smaller than those of other atoms. [S0163-1829(98)05447-2]

I. INTRODUCTION

Recently, much attention has been focused on column-III–nitride (III-N) compound semiconductors as a result of developments such as the blue-emitting laser diode and the light-emitting diode.[1] One of the prominent examples is the achievement of Nakamura *et al.*;[2] they recently reported an estimated lifetime of 10 000 h (about 1 year) for a continuous wave laser diode operating at room temperature. Although there have been many technological breakthroughs in this field,[1,3] relatively little is known for the fundamental physical properties of III-N semiconductors. For example, it is not well understood why nitride-based devices operate successfully in spite of ultrahigh unintentional background impurity concentrations for which GaAs-based devices can hardly operate.

The purpose of the present work is to study one of the basic physical properties of III-N semiconductors: the optical phonon, especially the optical-phonon-mode behavior in ternary semiconductors. Ternary semiconductors ($AB_{1-x}C_x$) are essential to realizing many physically important parameters necessary to achieve so-called bandgap engineering. Generally, optical-phonon characteristics in such ternary semiconductors can be categorized by three classes: one mode, two mode, and intermediate mode.[4] One-mode behavior exhibits only one set of longitudinal-optical (LO) and transversal-optical (TO) phonons whose frequencies vary almost linearly with compositional changes. Two-mode behavior exhibits two sets of phonons for each LO and TO phonon; each set is due to the lighter and heavier component of the two binary semiconductors that represent the compositional extremes of the ternary system. The intermediate-mode behavior exhibits two-mode behavior for a certain range of composition and one-mode behavior for the remaining compositional range. Phonons in $Ga_xAl_{1-x}As$ and $In_xGa_{1-x}As$ exhibit two-mode behavior, thus, the dielectric function for these ternary materials should be based on the two-pole model for accurate calculation.[5,6] Consequently, it is appropriate to understand the phonon-mode behavior in ternary III-N semiconductors ($Ga_xAl_{1-x}N$, $In_xGa_{1-x}N$, and etc.) before proceeding with calculations involving phonons. In this paper, the modified random-element isodisplacement (MREI) model[7] and the uniaxial model of Hayes and Loudon[8,9] are applied to III-N ternary material to determine the nature of the phonon modes in III-N ternary material.

II. MODIFIED RANDOM ELEMENT ISODISPLACEMENT MODEL

We adopt the MREI model for the ternary semiconductor $AB_{1-x}C_x$; the basic assumption of the MREI model is that a

fraction $(1-x)$ of B ions and a fraction x of C ions are the nearest neighbors of A ions. The long-range Coulomb interaction is included in the form of the local field. The advantage of using the MREI model is that this model does not require an *a priori* result—frequencies of gap or local modes—or an assumption as to whether the material is characterized by one-mode or two-mode behavior. This model requires only physical constants such as the atomic masses of the component atoms and the phonon frequencies of the two binary materials, which represent the compositional extremes of the ternary system.

The MREI model as explained in Ref. 7 assumes a crystal of cubic symmetry. However, the nitride-based semiconductor devices, such as blue laser diodes, are usually grown on a wurtzite structure. Hence, unlike the case of a cubic crystal, dielectric constants $(\epsilon_0, \epsilon_\infty)$, electronic polarizability (α), effective charge (e), and other physical constants must be treated not as scalars but as tensors. Since the wurtzite structure is the simplest within a uniaxial crystal, the governing tensor equations for optical phonons at the Γ point can be simplified into two uncoupled equations, i.e., components parallel (E_1 or Γ_5 branch) and perpendicular (A_1 or Γ_1 branch) to the c axis of the crystals.[8] It is noted that this macroscopic model, which utilizes the dielectric function, can only deal with the infrared-active phonons that contribute to the low frequency polarizability. Hence, other phonon branches in wurtzite crystals such as B or Γ_3 (silent) and E_2 or Γ_6 (Raman active) cannot be described by the MREI model.[8]

We have extended the MREI model to the case of wurtzite semiconductors. Considering only nearest-neighbor interactions, the phonon governing equations for wurtzite semiconductor $AB_{1-x}C_x$ in the long wavelength limit are given as follows:

$$m_A\ddot{u}_{Ai} = -(1-x)F_{bi}(u_{Ai}-u_{Bi}) - xF_{ci}(u_{Ai}-u_{Ci}) + \{(1-x)e_{bi}+xe_{ci}\}E_{\mathrm{loc},i}, \tag{1}$$

$$m_B\ddot{u}_{Bi} = -F_{bi}(u_{Bi}-u_{Ai}) - e_{bi}E_{\mathrm{loc},i}, \tag{2}$$

$$m_C\ddot{u}_{Ci} = -F_{ci}(u_{Ci}-u_{Ai}) - e_{ci}E_{\mathrm{loc},i}, \tag{3}$$

$$E_{\mathrm{loc},i} = E_i + \frac{4\pi}{3}\gamma_i P_i, \tag{4}$$

$$P_i = (1-x)\left\{\frac{e_{bi}}{v_b}(u_{Ai}-u_{Bi}) + \frac{\alpha_{Ai}+\alpha_{Bi}}{v_b}E_{\mathrm{loc},i}\right\}\frac{v_b}{v} + x\left\{\frac{e_{ci}}{v_c}(u_{Ai}-u_{Ci}) + \frac{\alpha_{Ai}+\alpha_{Ci}}{v_c}E_{\mathrm{loc},i}\right\}\frac{v_c}{v}, \tag{5}$$

where the subscript $i=\perp$ $(i=\parallel)$ corresponds to components perpendicular (parallel) to the c axis. The other subscripts b and c refer to binary materials AB and AC, respectively. Here, m and u_i are the mass and ith component of displacement of the ions A, B, and C. F_{bi} and F_{ci} are effective nearest-neighbor force constants, v is the volume of the unit cell of the mixed crystal while v_b and v_c are the unit cell volumes of the binary materials AB and AC, respectively. The dielectric function ϵ_i of the ternary semiconductor is defined by the usual expression between the macroscopic field E_i and the polarization P_i, i.e., $P_i=(\epsilon_i-1)E_i/4\pi$. The local field $E_{\mathrm{loc},i}$ deviates from the Lorentz relation, which is expressed by introducing γ_i. We take the ideal wurtzite structure values for γ_i from Ref. 10, i.e., $\gamma_\perp = 1+0.2\times(3/4\pi)$ and $\gamma_\parallel = 1-0.1\times(3/4\pi)$. Relations between microscopic and macroscopic parameters for the wurtzite crystal structure can be obtained by following the Born-Huang relation.[11] For crystal $AB(x=0)$,

$$\frac{4\pi}{3}\frac{\alpha_{Ai}+\alpha_{Bi}}{v_b} = \frac{\epsilon_{\infty bi}-1}{3+\gamma_i(\epsilon_{\infty bi}-1)}, \tag{6}$$

$$\frac{F_{bi}}{\mu_b} \equiv \omega_{Fbi}^2 = \frac{3+(\epsilon_{0bi}-1)\gamma_i}{3+(\epsilon_{\infty bi}-1)\gamma_i}\omega_{Tbi}^2, \tag{7}$$

$$\frac{4\pi}{3}\frac{e_{bi}^2}{\mu_b v_b} = \frac{3}{\gamma_i[3+\gamma_i(\epsilon_{\infty bi}-1)]}(\omega_{Fbi}^2-\omega_{Tbi}^2), \tag{8}$$

where μ_b is the reduced mass of crystal AB. ϵ_{0b}, $\epsilon_{\infty b}$, and ω_{Tb} are the static and high-frequency dielectric constant, and long-wavelength TO phonon frequency of the crystal AB, respectively. The above relations for crystal $AC(x=1)$ can be obtained by interchanging C with B and c with b.

The optical phonon frequencies ω_{Ti} and ω_{Li} of ternary $AB_{1-x}C_x$ semiconductor are obtained by solving Eqs. (1)–(5) simultaneously. The frequencies are given by the following roots:

$$\omega_{Xi}^2 = \frac{\Omega_{Xbi}^2+\Omega_{Xci}^2}{2} \pm \left[\left(\frac{\Omega_{Xbi}^2-\Omega_{Xci}^2}{2}\right)^2 + x(1-x)\Omega_{Xbci}^4\right]^{1/2}, \tag{9}$$

$$\Omega_{Xbi}^2 = \omega_{bi}^2 + (1-x)\beta_{Xi}\omega_{bi'}^2, \tag{10}$$

$$\Omega_{Xci}^2 = \omega_{ci}^2 + x\beta_{Xi}\omega_{ci'}^2, \tag{11}$$

$$\Omega_{Xbci}^4 = \left\{\left(\frac{\delta_{bi}}{\delta_{ci}}\right)^{1/2}\beta_{Xi}\omega_{bi'}\omega_{ci'} + \frac{\overline{\mu}}{m_A}\omega_{Fci}^2\right\} \times \left\{\left(\frac{\delta_{ci}}{\delta_{bi}}\right)^{1/2}\beta_{Xi}\omega_{bi'}\omega_{ci'} + \frac{\overline{\mu}}{m_A}\omega_{Fbi}^2\right\}, \tag{12}$$

where X stands for T and L, respectively, and β_{Xi} is $\beta_{Ti} = -\gamma_i$ for the transverse case and $\beta_{Li}=(3-\gamma_i)/\epsilon_{\infty i}$ for the longitudinal case. The explicit analytical expression for $\epsilon_{\infty i}$ of mixed crystal $AB_{1-x}C_x$ is

$$\frac{\epsilon_{\infty i}-1}{3+\gamma_i(\epsilon_{\infty i}-1)} = (1-x)\frac{v_b}{v}\frac{\epsilon_{\infty bi}-1}{3+\gamma_i(\epsilon_{\infty bi}-1)} + x\frac{v_c}{v}\frac{\epsilon_{\infty ci}-1}{3+\gamma_i(\epsilon_{\infty ci}-1)}, \tag{13}$$

which is the modified weighted Clausius-Mossotti relation. The static dielectric constant ϵ_{0i} is obtained from the Lyddane-Sachs-Teller relation, i.e., $\epsilon_{0i}=\epsilon_{\infty i}\omega_{Li}^2/\omega_{Ti}^2$. In the present work, we take $\epsilon_{\infty\perp}=\epsilon_{\infty z}$. This is quite a good assumption since ϵ_∞ is due primarily to electrons. The other quantities are given by

$$\omega_{bi}^2 = \omega_{Fbi}^2\left(1 - x\,\frac{\mu_b}{m_A}\right), \tag{14}$$

$$\omega_{bi'}^2 = \delta_{bi}\,\frac{v_b}{v}\,\frac{3+\gamma_i(\epsilon_{\infty i}-1)}{\gamma_i[3+\gamma_i(\epsilon_{\infty bi}-1)]}\,(\omega_{Fbi}^2\omega_{Tbi}^2), \tag{15}$$

$$\delta_{bi} = 1 - x\,\frac{\mu_b}{m_A}\left(1 - \frac{e_{ci}}{e_{bi}}\right), \tag{16}$$

$$\overline{\mu} = \sqrt{\mu_b \mu_c}. \tag{17}$$

The variables ω_{ci}, $\omega_{ci'}$, and δ_{ci} can be obtained by interchanging b by c and x by $(1-x)$ simultaneously in the equations given above. For simplicity, we assume δ_{bi}, δ_{ci}, v_b/v, and v_c/v to be one.[7] This assumption changes only the detailed curvature of phonon frequencies and the behavior of phonon mode is not affected.

The dielectric function $\epsilon_i(\omega)$ can be also obtained from Eqs. (1)–(5), that is,

$$\epsilon_i(\omega) = \epsilon_{\infty i}\,\frac{(\omega_{L+i}^2-\omega^2)(\omega_{L-i}^2-\omega^2)}{(\omega_{T+i}^2-\omega^2)(\omega_{T-i}^2-\omega^2)} = \epsilon_{\infty i} + \frac{f_{+i}\omega_{T+i}^2}{(\omega_{T+i}^2-\omega^2)} + \frac{f_{-i}\omega_{T-i}^2}{(\omega_{T-i}^2-\omega^2)}, \tag{18}$$

where the oscillator strength f_{+i} is given by

$$f_{+i}\omega_{T+i}^2 = \epsilon_{\infty i}\,\frac{(\omega_{L+i}^2-\omega_{T+i}^2)(\omega_{L-i}^2-\omega_{T+i}^2)}{(\omega_{T-i}^2-\omega_{T+i}^2)}. \tag{19}$$

The oscillator strength f_{-i} can be obtained by interchanging $+$ and $-$ in the equation shown above. The subscripts $+$ and $-$ correspond to the two solutions of ω_{Xi} in Eq. (9) by taking $(+)$ and $(-)$ signs, respectively. In order for the oscillator strengths to be positive, the order of the frequencies must satisfy the following inequality:[7]

$$\omega_{L+i} \geqslant \omega_{T+i} \geqslant \omega_{L-i} \geqslant \omega_{T-i}. \tag{20}$$

III. RESULTS AND DISCUSSION

Figure 1 indicates that $Ga_xAl_{1-x}N$ exhibits typical characteristics of one-mode behavior as illustrated in Ref. 7; i.e., no gap mode and local mode at the boundaries ($x=0$ and 1), almost linear dependence on compositional change, and large difference in oscillator strengths between the upper four strong modes, which take $(+)$ sign in Eq. (9) and the lower four weak modes, which take $(-)$ sign in Eq. (9). The total number of phonon branches is doubled as compared with cubic semiconductor crystals. This occurs as a result of the doubling of the number of equations for the wurtzite structure. Recent Raman experimental values for $Ga_xAl_{1-x}N$ are marked in Fig. 1.[12–14] The circles (squares) represent the measurement data for A_1 (E_1) modes of $Ga_xAl_{1-x}N$. For LO phonons, the theoretical and experimental results match relatively well. However, TO phonons show some discrepancy between the two. Considering the simplicity of MREI model and ignoring some factors, such as strain, our model gives a rather good prediction for phonon characteristics of wurtzite $Ga_xAl_{1-x}N$. Moreover, Demangeot *et al.*[12] have analyzed

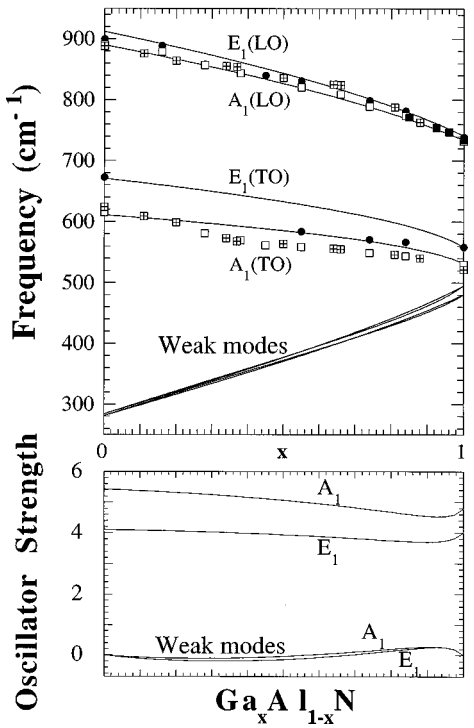

FIG. 1. (a) Optical phonon frequencies of E_1 and A_1 branches for $Ga_xAl_{1-x}N$ as a function of Ga composition x. Lower four curves below 500 cm^{-1} belong to the weak modes of E_1 and A_1 as mentioned in the text. Circles (squares) represent experimental values of E_1 (A_1) modes (filled circles and open squares, Ref. 12; squares with plus, Ref. 13; filled squares, Ref. 14). (b) Oscillator strengths as a function of x. The upper (lower) two curves correspond to the upper (lower) four curves of (a).

Raman data for the case of $Ga_xAl_{1-x}N$ using a generalized dielectric model for coupled LO modes and have obtained support for the apparent one-mode behavior of the polar LO phonons; the model adopted by these authors takes the total dielectric constant of $Ga_xAl_{1-x}N$ to be the composition-weighed sum of the dielectric constants for GaN and AlN.

As mentioned in Ref. 7, the lower four curves of Fig. 1(a), which take $(-)$ signs for ω_{Li} and ω_{Ti} in Eq. (9), are the weak modes where the two cations vibrate out of phase; thus, these modes have not yet been reported experimentally. This can be confirmed in Fig. 1(b), since their corresponding oscillator strengths represented by the lower two curves are virtually zero for all composition. The equations of the MREI model that determine the dispersion relations for the various phonon modes predict phonon frequencies for different modes that are nearly equal for a selected compositional range of the ternary wurtzite structures. For these compositional ranges, it is unclear that the assumed orderings of frequencies in the MREI model are valid. Furthermore, the weak modes of four curves are confined in a relatively small space. Thus, the ordering of the frequencies in Eq. (20), i.e., $\omega_{L-i} \geqslant \omega_{T-i}$, may not be fully guaranteed from this simple MREI model. As a consequence, the small negative values of the oscillator strengths in Fig. 1(b) are taken to mean only that the effective oscillator strength is small.

Figure 2 is a plot for the phonon dispersion curves for $In_xGa_{1-x}N$, which also indicates one-mode behavior. Since

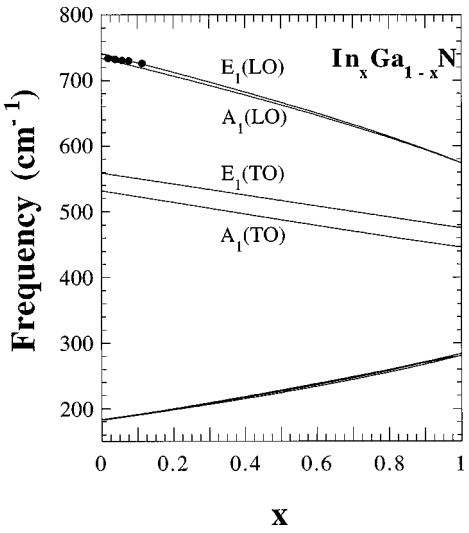

FIG. 2. Optical phonon frequencies of E_1 and A_1 branches for $In_xGa_{1-x}N$ as a function of In composition x. Lower four curves below 300 cm^{-1} are the weak modes of E_1 and A_1. Filled circles represent experimental data of E_1 (LO) modes from Ref. 18.

InN is hard to grow and its electron bandgap is readily available from by other materials, there has been relatively little attention given to binary InN.[15–17] The experimental values of E_1(LO) for $In_xGa_{1-x}N$ with In composition less than 11% are marked in the figure.[18] Although the oscillator strength plot for $In_xGa_{1-x}N$ is not shown here, it also exhibits almost the same features as $Ga_xAl_{1-x}N$. The parameters used in this calculation are summarized in Table I.

Some criteria have been proposed to determine the modal behavior of phonons in ternary semiconductors; in particular, these criteria distinguish between one-mode and two-mode behavior.[4,19] Since the atomic mass of nitrogen is much smaller than gallium, indium, and aluminum, the reduced masses of GaN, InN, and AlN are almost the same as that of N. This means that infrared-active optical-phonon vibrations in $In_xGa_{1-x}N$ and $Ga_xAl_{1-x}N$ are influenced strongly by the nitrogen atom. This observation is in accord with our results that A_1 and E_1 optical phonons of $Ga_xAl_{1-x}N$ and $In_xGa_{1-x}N$ exhibit one-mode behavior. Hence, for $Ga_xAl_{1-x}N$ and $In_xGa_{1-x}N$, more sophisticated criteria[19] or MREI models[20] may not be needed to specify the phonon-mode behavior, although a more detailed model could provide better fitting with experimental results. Due to the lack of good quality III-N ternary samples for a wide range of composition, it may be too early to compare the detailed phonon frequency profile between the theoretical and experimental work, especially for $In_xGa_{1-x}N$. Therefore, the main aim of this paper is not to seek a better fit to experimental results, but to find a theoretical framework for characterizing the phonon-mode behavior in the nitride ternary material.

TABLE I. Optical phonon frequencies (in cm^{-1}) and high-frequency dielectric constants used in the calculations.

	AlN	GaN	InN
$\hbar\omega(E_1,\mathrm{LO})$	912.0[a]	741.0[a]	574.0[b]
$\hbar\omega(A_1,\mathrm{LO})$	890.0[a]	734.0[a]	574.0[b]
$\hbar\omega(E_1,\mathrm{TO})$	670.8[a]	558.8[a]	475.0[b]
$\hbar\omega(A_1,\mathrm{TO})$	611.0[a]	531.8[a]	446.0[b]
ϵ_∞	4.84[c]	5.29[c]	8.40[d]

[a]Reference 21.
[b]Reference 16; the A_1(LO) and E_1(LO) peaks of InN are indistinguishable from each other in Raman experiments.
[c]Reference 22.
[d]Reference 23.

IV. CONCLUSION

We have calculated the phonon frequencies for the ternary nitride semiconductor over the entire compositional range. Based on an MREI model, it is found that optical phonons (A_1 and E_1) in $Ga_xAl_{1-x}N$ and $In_xGa_{1-x}N$ exhibit one-mode behavior unlike $Ga_xAl_{1-x}As$ and $In_xGa_{1-x}As$, which exhibit two-mode behavior. This result supports recent Raman experiments on $Ga_xAl_{1-x}N$.

ACKNOWLEDGMENTS

The authors gratefully acknowledge many fruitful discussions with Professor B. C. Lee. The authors are also thankful to Dr. Kwiseon Kim for informing them of recent theoretical and experimental data on InN. This work was supported, in part, by the U.S. Army Research Office and the Office of Naval Research.

[1] See, for example, S. Nakamura and G. Fasol, *The Blue Laser Diode* (Springer-Verlag, Berlin, 1997).
[2] S. Nakamura, M. Senoh, S. Nagahama, N. Iwasa, T. Yamada, T. Matsushita, H. Kiyoku, Y. Sugimoto, T. Kozaki, H. Umemoto, M. Sano, and K. Chocho, Jpn. J. Appl. Phys., Part 2 **36**, L1130 (1997).
[3] O.-H. Nam, M. D. Bremser, T. S. Zheleva, and R. F. Davis, Appl. Phys. Lett. **71**, 2638 (1997).
[4] I. F. Chang and S. S. Mitra, Adv. Phys. **20**, 359 (1971).
[5] K. W. Kim and M. A. Stroscio, J. Appl. Phys. **68**, 6289 (1990).
[6] S. Yu, K. W. Kim, M. A. Stroscio, G. J. Iafrate, J.-P. Sun, and G. I. Haddad, J. Appl. Phys. **82**, 3363 (1997).
[7] L. Genzel, T. T. Martin, and C. H. Perry, Phys. Status Solidi B **62**, 83 (1974).
[8] W. Hayes and R. Loudon, *Scattering of Light by Crystals* (Wiley, New York, 1978), p. 149.
[9] B. C. Lee, K. W. Kim, M. Dutta, and M. A. Stroscio, Phys. Rev. B **56**, 997 (1997).
[10] H. W. Verleur and A. S. Barker, Jr., Phys. Rev. **155**, 750 (1967).
[11] M. Born and K. Huang, *Dynamical Theory of Crystal Lattices* (Clarendon, Oxford, 1954), p. 82.
[12] F. Demangeot, J. Groenen, J. Frandon, M. A. Renucci, O. Briot, S. Clur, and R. L. Aulombard, Appl. Phys. Lett. **72**, 2674 (1998).

[13] A. Cros, H. Angerer, R. Handschuh, O. Ambacher, M. Stutzmann, MRS Internet J. Nitride Semicond. Res. **2**, 43 (1997) (available from http://nsr.mij.mrs.org/2/43).

[14] D. Behr, R. Niebuhr, J. Wagner, K.-H. Bachem, and U. Kaufmann, Appl. Phys. Lett. **70**, 363 (1997).

[15] K. Kim, W. R. L. Lambrecht, and B. Begall, Phys. Rev. B **53**, 16 310 (1996); **56**, 7018 (1997).

[16] J. S. Dyck, K. Kash, K. Kim, W. R. L. Lambrecht, C. C. Hayman, A. Argoitia, M. T. Grossner, W. L. Zhou, and J. C. Angus, in *Nitride Semiconductors*, edited by S. DenBaars, B. Meyer, S. Nakamura, F. Ponce, and T. Strite, MRS Symposia Proceedings No. 482 (Materials Research Society, Pittsburgh, 1998), p. 549.

[17] H.-J. Kwon, Y.-H. Lee, O. Miki, H. Yamano, and A. Yoshida, Appl. Phys. Lett. **69**, 937 (1996).

[18] D. Behr, R. Niebuhr, J. Wagner, K. H. Bachem, and U. Kaufmann, in *Gallium Nitride and Related Materials II*, edited by C. R. Abernathy, H. Amano, and J. C. Zolper (Materials Research Society, Pittsburgh, 1997), p. 213.

[19] H. Harada and S. Narita, J. Phys. Soc. Jpn. **30**, 1628 (1971).

[20] P. D. Lao, Y. Guo, G. G. Siu, and S. C. Shen, Phys. Rev. B **48**, 11 701 (1993).

[21] V. Yu. Davydov, Yu. E. Kitaev, I. N. Goncharuk, A. O. Lebedev, A. N. Smirnov, A. M. Tsaregordtsev, M. B. Smirnov, A. P. Mirgorodskii, and O. K. Semchinova, in *Nanostructures: Physics and Technology*, edited by Zh. Alferov and L. Esaki (Ioffe Physico-Technical Institute, St. Petersburg, 1997), p. 244.

[22] *Numerical Data and Functional Relationships in Science and Technology*, Landolt-Börnstein New Series Group III, Vol. 17 (Springer, New York, 1982), pp. 159–182.

[23] T. L. Tansley, in *Properties of Group III Nitrides*, edited by J. H. Edgar (INSPEC, London, 1994), p. 35.